MULTI-BAND CIRCULARLY POLARIZED ANTENNA FOR WIRELESS APPLICATIONS

Ajith kumar V[1], Balaji D[2], Ashok P[3]

[1] *Department of ECE, PSVP Engineering College,Tamilnadu,India*
[2] *Department of ECE, PSVP Engineering College,Tamilnadu,India*
[3] *Assistant Professor,Department of ECE, PSVP Engineering College,Tamilnadu,India*

ABSTRACT

A quad-band circularly polarized (CP) antenna for 2.4/5.3/5.8 GHz WLAN and 3.5 GHz WiMAX applications is proposed. Three CP modes operating at the 2.4/3.5/5.8 GHz frequency bands are first achieved by a patch antenna composed of an inverted-U-shaped radiator with additional I-shaped and L-shaped strips, all rotated by 45^o around the horizontal axis. By placing a simple frequency selective surface (FSS) of 6× 6 square metallic patches under this antenna, 5.3 GHz linearly polarized (LP) signals are converted into CP signals, producing a quad-band CP antenna. Thus, such antennas that are compact and have multiband capability can be promising candidates for many wireless applications. Now in this slotted multi band planar system is proposed to intend on working on for frequency bands such as IN GPS, WLAN (over two frequency band spectrum), and Wi-MAX.

Keyword : - *Microstrip antenna,Circularly polarized antenna, Multi band antenna,Frequency selective surface, CST, Wireless networks.*

1. INTRODUCTION

Along the ongoing development of various wireless communication applications, multi-functional antenna systems have become more essential for the next-generation communication systems where several wireless communication applications such as Wireless Local Area Network (WLAN: 2.4–2.484, 5.15–5.25, 5.25–5.35, 5.47–5.725 and 5.725–5.850 GHz) and Worldwide Interoperability for Microwave Access (WiMAX: 2.5–2.69, 3.40–3.69 and 5.25–5.85 GHz) are required to operate simultaneously. Several countries around the world such as United States, Canada, Italy, Poland, Spain and Australia have already used both WLAN and WiMAX technologies to provide wireless high-speed Internet and network connections. Furthermore, circularly polarized (CP) antennas, with their distinct advantages over linearly polarized (LP) antennas, have been widely used in modern wireless communication systems [1]. Therefore, a single antenna with multi-band CP characteristics has received great attention, and various multi-band or broadband antennas have been presented [2-7]. However, these antennas either did not achieve CP caracteristics [2] or achieved them only for partial bands [3-7]. Recently, metamaterial structures have been applied to antennas to enhance their CP radiation characteristics. In [8], CP radiation from a patch antenna was improved by the use of a reactive impedance surface (RIS) layer. In other reports, metasurface (MS) structures were used to convert LP signals into CP signals [9, 10].

In this work, a quad-band CP antenna for 2.4/5.3/5.8 GHz WLAN and 3.5 GHz WiMAX applications is presented. Three CP modes operating at the 2.4/3.5/5.8GHz frequency bands are first achieved by a patch antenna composed of an inverted-U-shaped radiator with additional I-shaped and L-shaped strips, all rotated by 45^o around the horizontal axis. Next, by placing a simple frequency selective surface (FSS) of 6 × 6 square metallic patches under this antenna, LP signals at the 5.3 GHz WLAN band are converted into CP signals, producing a quad-band CP antenna. To the best of the authors' knowledge, no antenna has ever achieved quad-band CP characteristics for

WLAN and/or WiMAX applications so far.

2. ANTENNA DESIGN

This section describes the design process of the proposed antenna in three steps. First, a triple-band CP patch antenna similar to that in [7] is designed on a Taconic RF-5 substrate with thickness of 1.52 mm, a dielectric constant of 2.2 and a loss tangent of 0.0009. Next, a metallic FSS unit cell is implemented by investigating the reflection phase characteristics at the 5.3 GHz WLAN band. Finally, the patch antenna is suspended at a height of H above the FSS composed of 36 unit cells in a 6 × 6 layout on a Taconic RF-35 substrate with thickness of 1.52 mm, a dielectric constant of 3.5 and a loss tangent of 0.0018. The horizontal distance between the bottom edges of the antenna substrate and the FSS substrate is L. Fig. 1 shows the geometry of the antenna with the final optimized dimensions.

2.1 Triple band CP patch antenna

The overall view of the triple-band CP patch antenna is shown in Fig. 1(c). The final optimized geometry was obtained through simulations with the software CST as reported in [7]. Three CP modes operating at the 2.4/3.5/5.8 GHz frequency bands were achieved using an inverted-U-shaped radiator with additional I-shaped and L-shaped strips, all rotated by 45^{o} around the axis. The simulation of the microstrip patch antenna design system was established by using the Computer Simulation Technology (CST) . The simulation of the important two parameter as reflection coefficient (S11) and the axial ratio (AR) are shown in Fig. 2.

]

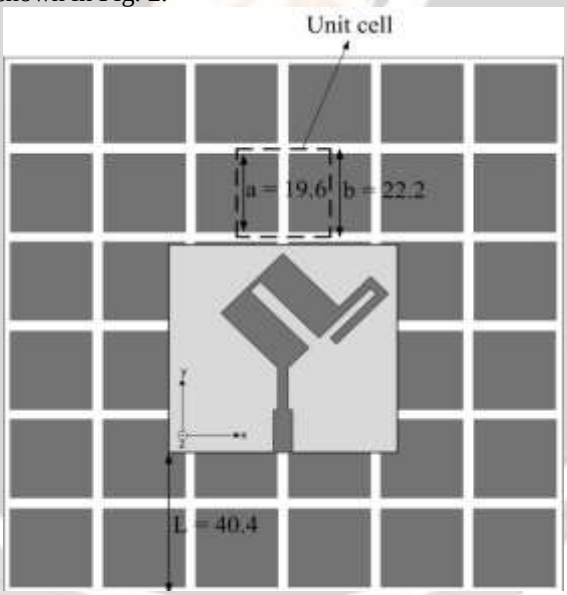

(a)

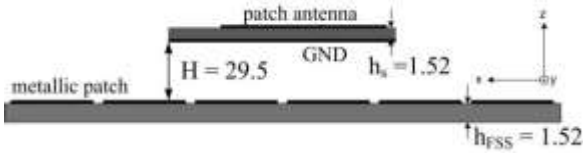

(b)

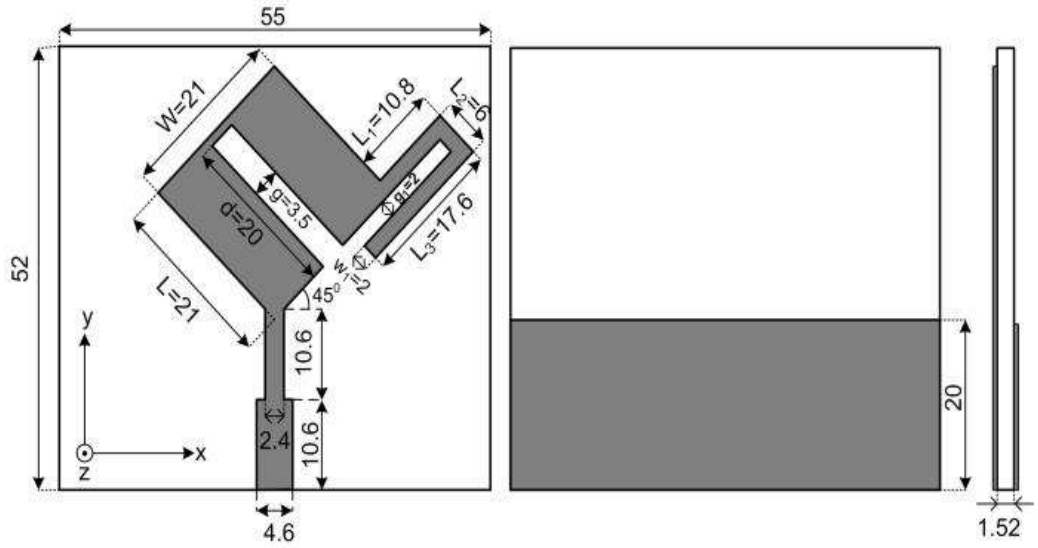

(c)

Fig -1: Geometry of the proposed quad-band circularly polarized (CP) antenna
(a) top view, (b) side view and (c) triple-band CP antenna (units in millimetres).

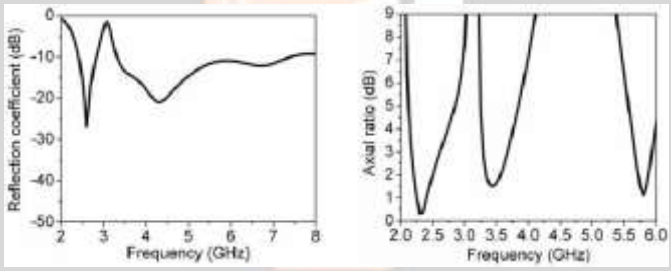

Fig -2: Simulated characteristics of the triple-band CP antenna (a) reflection coefficient and (b) AR

2.2 FSS unit cell

An important parameter in the investigation of the FSS as well as other metamaterial structures is the resonant frequency. The resonant frequency of the FSS is defined as the frequency at which the reflection phase is equal to 0^o, and the bandwidth of the FSS is defined for the reflection phase between $+90^o$ and -90^o [11]. To determine the reflection phase of the FSS, a FSS unit cell was optimized by placing one cell in the computational domain of CST [12]. The sizes of the square metal patch and the square unit cell are denoted by a and b respectively. A waveport exciting the propagating plane wave was placed at 28.3 mm above the FSS, approximately one-half wavelength at the resonant frequency of 5.3 GHz, and de-embedded on the FSS. The desired operating frequency band was tuned between the PEC (reflection phase of 180°) and the PMC (reflection phase of 0°). After optimization, a and b were determined to be 19.6 mm and 22.2 mm respectively. The reflection phase of the unit cell lies between $+90^o$ and -90^o in the frequency range of 5.25–5.35 GHz, with a resonant frequency of 5.3 GHz.

2.3 Triple-band CP patch antenna on FSS

The triple-band CP patch antenna was first placed at a distance of 28.3 mm above the center of the FSS, and antenna characteristics for different number of unit cells were studied. As a result, a FSS structure consisting of 6 × 6 metal patches periodical along the x- and y-axis was determined to give the best results. Finally, the

dimensions of the FSS and the position of the antenna relative to the FSS were further optimized to provide the best quad-band CP characteristics at the intended frequencies of 2.4/3.5/5.3/5.8 GHz. The final optimized values are shown in Fig. 1(a) and 1(b). The total size of the FSS is 133.2 × 133.2 mm^2. Parametric studies are provided in Fig. 3 to Fig. 6 to investigate the effect of the design parameters on the antenna characteristics. Fig. 3 shows the influence of a, the size of the square metal patch, on the CP bands. It is observed that the reflection coefficients change only slightly, while the CP characteristics change significantly. It affects both the resonant frequency and the CP frequencies of the two upper bands near 5.3 GHz and 5.8 GHz without affecting the antenna performance at 2.4 GHz and 3.5 GHz. As a is increased, both upper CP bands tend to shift to the lower frequency region. The size of the square unit cell, b, also shows similar influence on the CP bands. The effect of the array size is investigated in Fig. 4, showing the best quad-band CP radiation using the 6 × 6 cell configuration. The influence of H, the vertical position of the antenna above the FSS, is investigated in Fig. 5. Large changes are observed in both the reflection coefficient and the AR characteristics. Increasing or decreasing H causes shifting of the CP bands to unintended frequencies and reduction of both the impedance and the AR bandwidth. Finally, the effect of L, the horizontal position of the antenna relative to the FSS, is investigated in Fig. 6, showing large influence on the AR characteristics at 2.4, 5.3 and 5.8 GHz.

The effect of the FSS in creating the fourth CP band can be explained as follows. When a LP antenna is placed over the FSS with different reflection phases of +90° and –90° along the x- and y-axis, the total radiated field in the +z-direction, where is the direct radiated field by the antenna and is the reflected field by the FSS [13]. The reflected field becomes perpendicular to the radiated field with 90° phase difference, thus a CP radiation pattern is obtained.

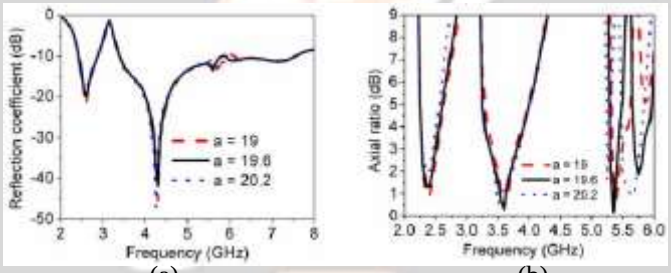

(a) (b)

Fig -3: Simulated (a) reflection coefficient and (b) AR with various sizes of the square metal patch.

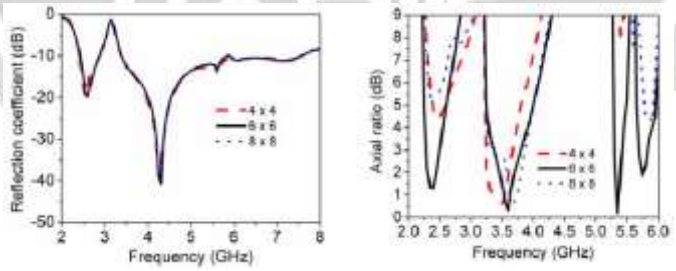

(a) (b)

Fig -4: Simulated (a) reflection coefficient and (b) AR with various numbers of unit cells.

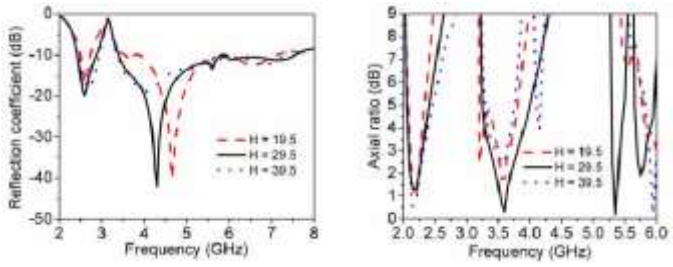

(a) (b)

Fig -5: Simulated (a) reflection coefficient and (b) AR with various vertical positions of the patch antenna.

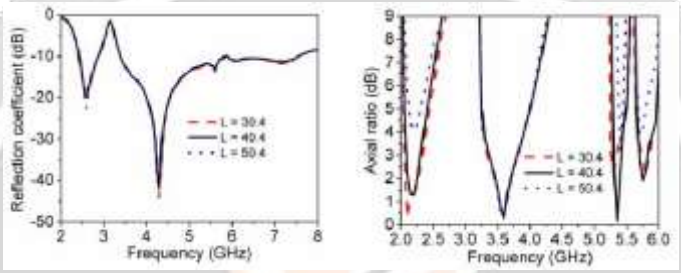

(a) (b)

Fig -6: Simulated (a) reflection coefficient and (b) AR with various horizontal positions of the patch antenna.

To visualize the CP operation of the antenna, the current distribution on the triple-band CP patch antenna with and without the FSS are simulated in Fig. 7 at 5.3 GHz for t = 0 and t = T/4, where T is the period. When the antenna is placed in free space, the vector sum of the major current components at t = 0 (Jsum1) is orthogonal to that at t = T/4 (Jsum2), but the magnitude of Jsum1 is greater than that of Jsum2. Therefore, CP mode cannot be created. In contrast, when the antenna is placed over the FSS, Jsum1 is orthogonal to Jsum2 and the magnitude of Jsum1 is similar to that of Jsum2. Thus CP mode can be achieved.

3. MEASUREMENT RESULT

The photograph of the fabricated quad-band CP antenna is presented in Fig. 8. The antenna substrate is placed above the FSS using four small foam supports at the corners. The simulated and measured reflection coefficient and the AR characteristics are shown in Fig. 9. Measured and simulated results show good agreement, with slight discrepancies attributed to the fabrication tolerances and the approximate boundary conditions used in the computational domain. The antenna has successfully achieved a quad-band CP operation for 2.4/5.3/5.8 GHz WLAN and 3.5 GHz WiMAX applications. The antenna exhibits a measured –10 dB impedance bandwidth of 380 MHz (2.37–2.75 GHz) and 4.6 GHz (3.4–8 GHz). The measured 3dB AR bandwidth is 5.4% (2.35–2.48 GHz), 8.3% (3.45–3.75 GHz), 3.7% (5.25–5.45 GHz), and 2.9% (5.7–5.87 GHz) respectively. Thus, such antennas that are compact and have multiband capability can be promising candidates for many wireless applications. Now in this slotted multi band planar system is proposed to intend on working on for frequency bands such as IN GPS, WLAN (over two frequency band spectrum), and Wi-MAX.

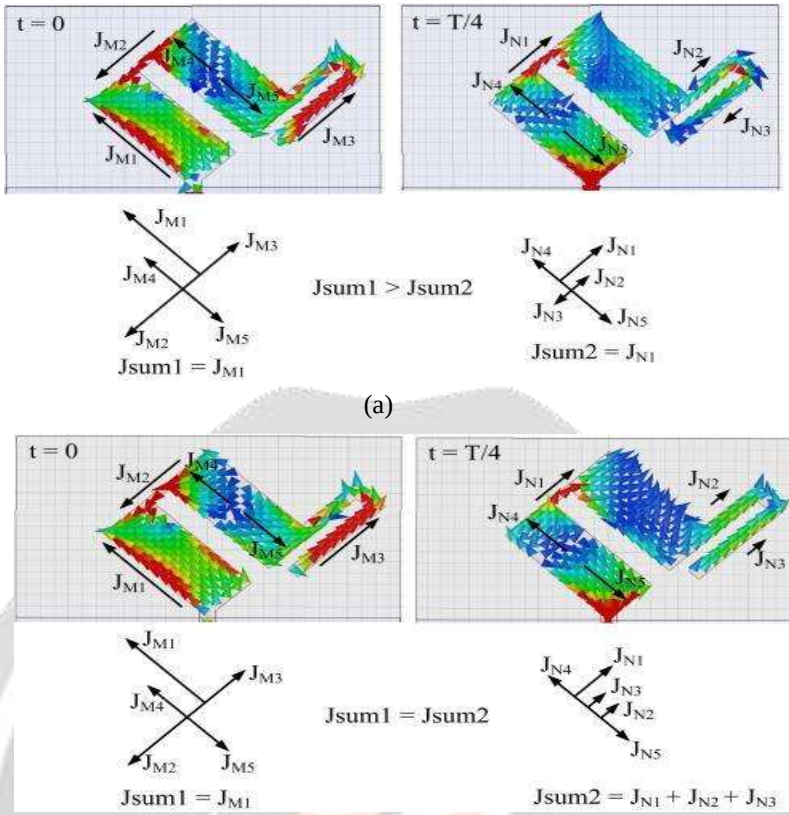

Fig -7: Simulated current distribution (a) without FSS and (b) with FSS at 5.3 GHz for t = 0 and t = T/4.

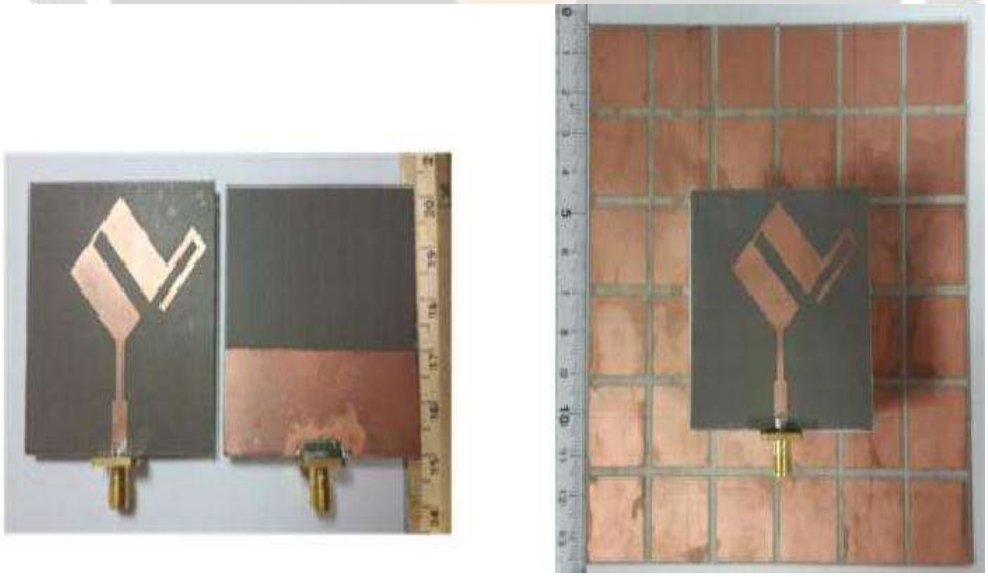

(a) (b)

Fig -8: Photograph of (a) the triple-band CP antenna and (b) the quad-band CP antenna

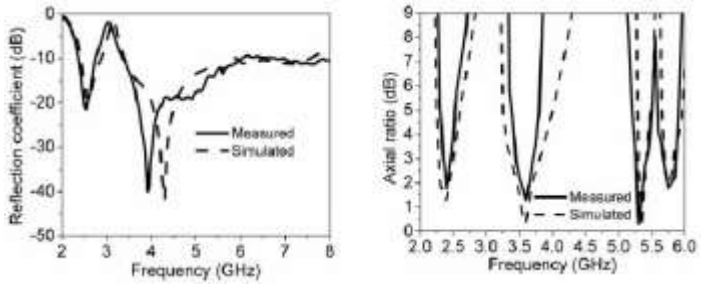

(a) (b)

Fig -9: . Measured and simulated (a) reflection coefficient and (b) AR of the quad-band CP antenna.

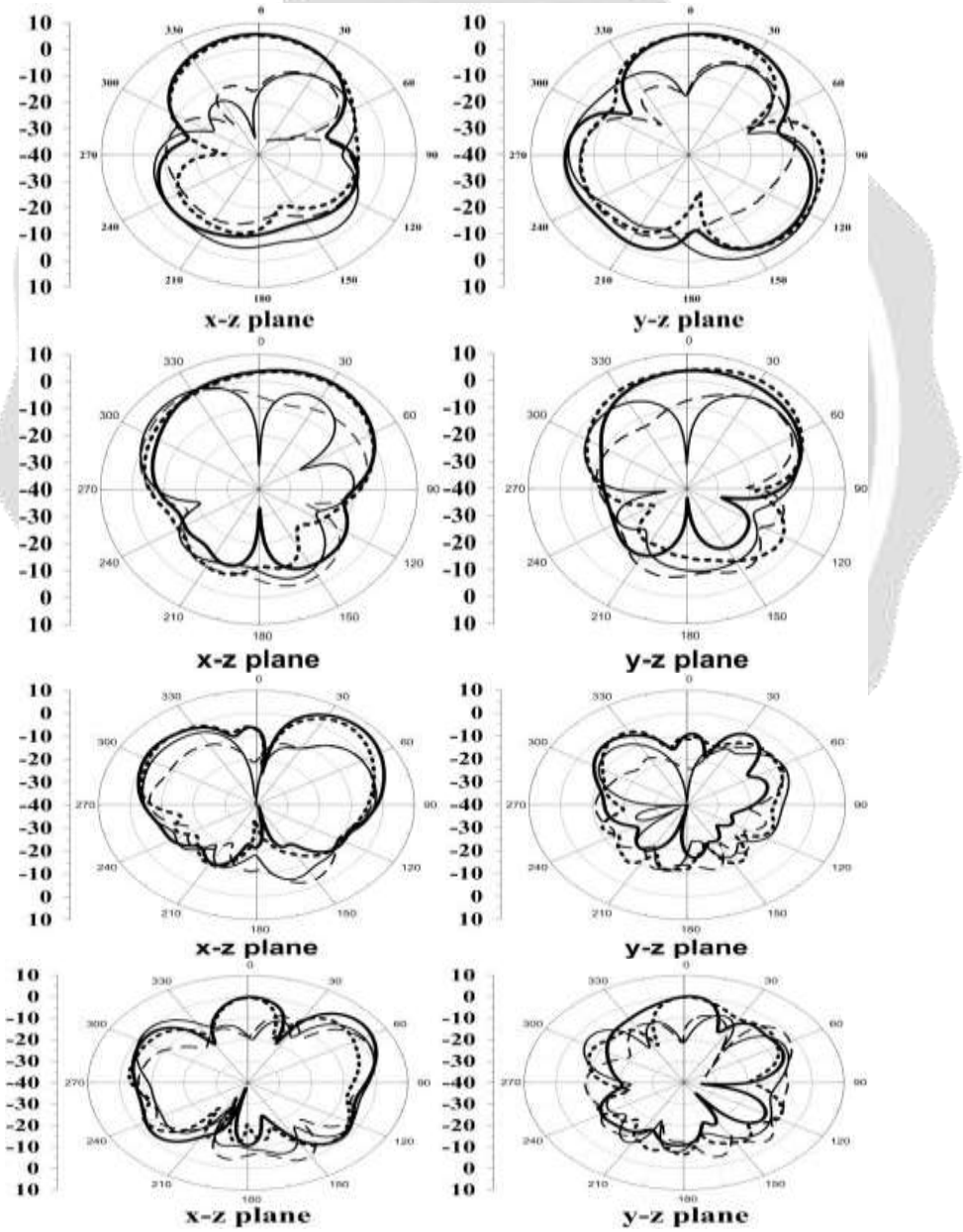

Fig -10: . Measured and simulated normalized radiation patterns of the quad-band antenna for the principal planes

(x–z and y–z) at (a) 2.4 GHz, (b) 3.5 GHz, (c) 5.3 GHz and (d) 5.8 GHz.

Fig. 10 shows the simulated and measured far-field radiation patterns in the x-z and y-z planes at the frequencies of 2.4, 3.5, 5.3 and 5.8 GHz. They are mainly LHCP for z > 0. All the measured results are within reasonable agreement with the simulation results. At 2.4, 3.5, 5.3 and 5.8 GHz, the measurements yielded a gain of 5.95, 6.92, 6.37 and 6.07 dBic respectively. Additionally, the measured radiation efficiencies were 82.13, 82.61, 94.11 and 95.12% respectively.

4. CONCLUSIONS

A quad-band circularly polarized antenna for 2.4/5.3/5.8 GHz WLAN and 3.5 GHz WiMAX applications was proposed, fabricated and characterized. Three CP modes at 2.4/3.5/5.8 GHz were achieved by a patch antenna composed of an inverted-U-shaped radiator with additional I-shaped and L-shaped strips, all rotated by 45^{o} around the horizontal axis. Next, by placing a simple FSS structure under this antenna, an additional CP mode at 5.3 GHz was achieved. The demonstrated antenna showed measured 3dB axial-ratio bandwidth of 5.4% (2.35–2.48 GHz), 8.3% (3.45–3.75 GHz), 3.7% (5.25–5.45 GHz), and 2.9% (5.7–5.87 GHz).

5. REFERENCES

[1] S. Gao, Q. Luo, and F. Zhu, “Circularly polarized antennas,” Wiley-IEEE Press, New York, November 2013.

[2] S. Verma and P. Kumar, “Compact triple-band antenna for WiMAX and WLAN applications,” Electron. Lett., vol. 50, no. 7, pp. 484–486, 2014.

[3] T. Wu, X. W. Shi, P. Li, and H. Bai, “Tri-band microstrip-fed monopole antenna with dual-polarisation characteristics for WLAN and WiMAX applications,” Electron. Lett., vol. 49, no. 25, pp. 1597–1598, 2013.

[4] T. T. Le and H. C. Park, “Very simple circularly polarised printed patch antenna with enhanced bandwidth,” Electron. Lett., vol. 50, no. 25, pp. 1896–1898, 2014.

[5] J. G. Baek and K. C. Hwang, “Triple-band unidirectional circularly polarized hexagonal slot antenna with multiple L-shaped slits,” IEEE Trans. Antennas Propag., vol. 61, no. 9, pp. 4831–4835, 2013.

[6] X. L. Bao and M. J. Ammann, “Printed triple-band circularly polarised antenna for wireless systems,” Electron. Lett., vol. 50, no. 23, pp. 1664–1665, 2014.

[7] T. V. Hoang and H. C. Park, “Very simple 2.45/3.5/5.8 GHz triple-band circularly polarised printed monopole antenna with bandwidth enhancement,” Electron. Lett., vol. 50, no. 24, pp. 1792–1793, 2014.

[8] K. Agarwal, Nasimuddin, and A. Alphones, “RIS-Based compact circularly polarized mircostrip antennas,”IEEE Trans. Antennas Propag., vol. 61, no. 2, pp. 547–554, 2013.

[9] K. Agarwal, Nasimuddin, and A. Alphones, “Triple-band compact circularly polarised stacked microstrip antenna over reactive impedance meta-surface for GPS applications,” IET Microw. Antennas Propag., vol. 8, no. 13, pp. 1057–1065, 2014.

[10] H. L. Zhu, S. W. Cheung, K. L. Chung, and T. I. Yuk, “Linear-to-circular polarization conversion using metasurface,” IEEE Trans. Antennas Propag., vol. 61, no. 9, pp. 4615–4623, 2013.

[11] S. Clavijo, R. E. Diaz, and W. E. McKinzie, “Design methodology for sievenpiper high-impedance surfaces: An artificial magnetic conductor for positive gain electrically small antennas,” IEEE Trans. Antennas Propag., vol. 51, no. 10, pp. 2678–2690, 2003.

[12] A. E. I. Lamminen, A. R. Vimpari, andJ. Saily, “UC-EBG on LTCC for 60-GHz frequency band antenna applications,” IEEE Trans. Antennas Propag., vol. 57, no. 10, pp. 2904–2912, 2009.

[13] F. Yang and Y. Rahmat-Samii, “A low profile single dipole antenna radiating circularly polarized waves,” IEEE Trans. Antennas Propag., vol. 53, no. 9, pp. 3083–3086, 2005.